https://doi.org/10.5194/egusphere-2022-332
Preprint. Discussion started: 30 May 2022

Sensitivity of Heinrich-type ice-sheet surge characteristics to boundary forcing perturbations

Clemens Schannwell[1], Uwe Mikolajewicz[1], Florian Ziemen[2], and Marie-Luise Kapsch[1]

[1]Max Planck Institute for Meteorology, Bundesstraße 53, 20146 Hamburg, Germany
[2]Deutsches Klimarechenzentrum, Bundesstr. 45a, 20146 Hamburg, Germany

Correspondence: Clemens Schannwell (Clemens.Schannwell@mpimet.mpg.de)

Abstract. Heinrich-type ice-sheet surges are one of the dominant signals of glacial climate variability. They are characterised as abrupt, quasi-periodic episodes of ice-sheet instabilities during which large amounts of ice are discharged from ice sheets into the ocean. The occurence of ice-sheet surges strongly influences the global climate evolution by altering the ocean circulation through the addition of freshwater and the atmospheric circulation through changes in ice-sheet height. The mechanisms controlling the timing and occurence of Heinrich-type ice-sheet surges remain poorly constrained to this day. Here, we use a coupled ice sheet-solid earth model to identify and quantify the importance of boundary forcing for the surge cycle length of Heinrich-type ice-sheet surges for two prominent ice streams of the Laurentide ice sheet - the land-terminating Mackenzie ice stream and the marine-terminating Hudson ice stream. We show that surface mass balance perturbations have the largest effect on the surge cycle length. Pertubations to the ice surface temperature and geothermal heatflux also influence the surge cycle length, but to a lesser degree. Ocean and sea-level forcing as well as different frequencies of the same forcing have a negligible effect on the surge cycle length. The simulations also highlight that only a certain parameter space exists under which ice-sheet oscillations can be maintained. Transitioning from an oscillatory state to a persistent ice streaming state, can result in an ice volume loss of up to 26% for the respective ice stream drainage basin under otherwise constant climate conditions. We show that Mackenzie ice stream is susceptible to undergoing such a transition in response to all tested positive climate perturbations. This underlines the potential of the Mackenzie region to have contributed to prominent abrupt climate change events of the last deglaciation.

1 Introduction

Heinrich-type ice-sheet surges (Heinrich, 1988, henceforth: surges or ice-sheet surges) are among the most dominant signals of glacial climate variability. Many hypotheses on what initiates such events have been proposed over the last decades (e.g. MacAyeal, 1993; Hulbe et al., 2004; Álvarez-Solas et al., 2011; Bassis et al., 2017). Early theories suggest that the surges are a result of internal ice-sheet oscillations that follow a two-stage pattern in which the ice sheet builds up (binge phase) and subsequently surges (purge phase, MacAyeal (1993)). However, this mechanism has been questioned because most of the documented ice-sheet surges fall into the cold stadials of Dansgaard-Oeschger (DO) cycles (Bond et al., 1993), indicating that a common climatic trigger exists. In the first ice-sheet surge simulation of Hudson ice stream with a 3D ice-sheet model,

https://doi.org/10.5194/egusphere-2022-332
Preprint. Discussion started: 30 May 2022

Calov et al. (2002) reproduced ice-sheet surges during cold DO stadials by applying a weak sliding peturbation with a 1,500 year period to a small region at the snout of the Hudson ice stream. This implicated the ocean as potential trigger of ice sheet surges that has been supported by proxy data showing an ocean warming signal prior to surge events (Marcott et al., 2011). As a result, varying hypotheses identifying the ocean as the key driver for triggering ice-sheet surges have been proposed (e.g. Álvarez-Solas et al., 2011; Marcott et al., 2011; Bassis et al., 2017). Some studies suggest that the increase in ocean temperatures at the ice-ocean interface may have caused the disintegration of a large ice shelf between the Laurentide and Greenland ice sheet (e.g Hulbe et al., 2004; Alvarez-Solas et al., 2013). The sudden removal of the stabilising ice shelf initiates the surge similar to the recent collapse of Larsen B ice shelf and the subsequent speed-up observed of the ice streams in the Antarctic Peninsula region (e.g. Rignot et al., 2004). While this could explain the timing of the surge events during the cold stadials, there is a lack of evidence about the existence of an ice shelf in the reconstructions prior to several recorded surge events (e.g. de Vernal et al., 2000). More recent theories propose that warm water intrusions onto the continental shelf in combination with a retrograde sloping subglacial topography trigger widespread ice-sheet retreat (Bassis et al., 2017). Subsequent glacial isostatic uplift cuts off the passage of the warm ocean water onto the continental shelf, leading to a re-advance of the ice sheet. The recent observed widespread retreat of tidewater glacier in Greenland has also been attributed to the intrusion of warm ocean waters into the fjords (e.g. Straneo and Heimbach, 2013; Murray et al., 2015). Until now, the Ice-Sheet Model Intercomparison Project–Heinrich Event INtercOmparison (ISMIP HEINO) has provided the only attempt to investigate the sensitivity of ice-sheet surges to different boundary forcing perturbations (Calov et al., 2010), showing that the surge behaviour with an idealised ice sheet is highly model and parameter dependent.

In addition to their importance for ice-sheet dynamics, ice-sheet surges of the Hudson ice stream also have a notable effect on the evolution of the global climate as shown by proxy data (e.g. Bond et al., 1993; Broecker, 1994; de Vernal et al., 2000) as well as coupled climate simulations (e.g. Roberts et al., 2014; Ziemen et al., 2019). In the model simulations, the associated climate response follows a two-stage pattern. During the surge, the freshwater discharge into the ocean leads to a strong cooling and reduction of ocean heat release over the North Atlantic (Ziemen et al., 2019). The freshening of the ocean leads to reduced North Atlantic deepwater formation and thus a weakening of the Atlantic Meridional Overturning Circulation (AMOC). After the termination of the surge, the reduced surface elevation of the ice sheet dominates changes in the atmospheric circulation. A lower Laurentide ice sheet results in a northward shift of the jet stream that reduces the northward transport of warm subtropical water to high latitudes, where it leads to a cooling (Ziemen et al., 2019). The timing and location of the freshwater input also bears significance for the ocean and climate response as shown by several freshwater perturbation experiments (Maier-Reimer and Mikolajewicz, 1989; Schiller et al., 1997; Stouffer et al., 2006; Smith and Gregory, 2009; Lohmann et al., 2020). A direct link between freshwater input from ice-sheet surges and abrupt climate change events (e.g. Meltwater Pulse 1a, Younger Dryas cold period) during the last deglaciation has been indicated by several studies (Maier-Reimer and Mikolajewicz, 1989; Broecker et al., 1989; Tarasov and Peltier, 2005; Condron and Winsor, 2012; Lin et al., 2021).

In this study, the key objective is to identify important external forcings and boundary conditions and quantify their effect on the timing and frequency of ice-sheet surges. We use an ensemble of coupled ice sheet-solid earth simulations and focus our simulations on two regions of the Laurentide ice sheet - the land-terminating Mackenzie ice stream and the marine-terminating

https://doi.org/10.5194/egusphere-2022-332
Preprint. Discussion started: 30 May 2022

Hudson ice stream (Fig. 1). To address these questions, we perform three different types of experiments. The first category investigates the response of time-invariant anomaly peturbations to the surface mass balance (SMB), geothermal heatflux, ice surface temperature, and sea-level on the surge characteristics. The second category studies the effect of different frequency forcing of the SMB and glacial isostatic adjustment (GIA) on the surge characteristics in comparison to time-invariant forcing. The third type of experiment investigates the interactions between the different surge areas by artificially suppressing surging in one of the surge regions. Our experiments are similar in spirit to Calov et al. (2010), but we extend their study by using a coupled ice sheet-solid earth model, perform a richer set of sensitivity experiments, employ a more sophisticated ice-sheet model at higher horizontal resolution, and simulate real-world ice stream geometries in different glaciological settings.

The paper is structured as follows. Section 2 introduces the coupled model setup, initial state as well as how the idealised climate forcing is generated. In section 3, we first discuss the surge behaviour of the two regions in the Ctrl simulation with constant forcing, before we detail the differences in the surge mechanism between the land-terminating Mackenzie ice stream and the marine-terminating Hudson ice stream. Subsequently, the sensitivities of the ice sheet surges are presented and interpreted in context of the different ice stream characteristics. Finally, section 4 summarises the main findings.

2 Methods

Proxy data show that most Heinrich and DO events during the last glacial cylce occurred during Marine Isotope Stage 3 (MIS3; North Greenland Ice Core Project members, 2004). Therefore, we use MIS3 climate conditions for our ice sheet-solid earth simulations. By identifying and combining three ice-sheet surge events from a MIS3 simulation with an Earth System Model (ESM) that includes interactive ice-sheet and solid-earth components, we generate an idealised climate forcing that allows for the explicit modelling of Heinrich-type ice-sheet surges. In the following, we describe the model setup, initial state, and the generation of the idealised composite forcing in more detail.

2.1 Model setup and initial state

The coupled ice sheet-solid earth model mPISM-VILMA, consisting of the modified Parallel Ice Sheet Model (mPISM, Ziemen et al., 2014, 2019) and the global VIscoelastic Lithosphere and MAntle model (VILMA, Martinec et al., 2018) is employed for our simulations. VILMA computes the solid-Earth deformation and the change in relative sea level caused by a redistribution of ice and water. We use VILMA in its 1D configuration, implicitly assuming that the solid-Earth structures only vary with depth, but are otherwise spatially homogeneous. mPISM is employed to compute the ice-sheet response. An earlier version of mPISM has been successfully applied in previous simulations of ice-sheet surges (e.g. Ziemen et al., 2019).

To compute ice velocities, mPISM (Ziemen et al., 2014) uses a simple addition of the Shallow Ice Approximation (SIA) and Shallow Shelf Approximation (SSA) ice velocities. Basal melt under floating ice shelves is calculated from ocean temperature and ocean salinity following the three-equation method of Holland and Jenkins (1999). The differences in the model setup that go beyond changes in the base versions of MPI-ESM and PISM, and the methods employed in the coupling, are described in the following.

https://doi.org/10.5194/egusphere-2022-332
Preprint. Discussion started: 30 May 2022

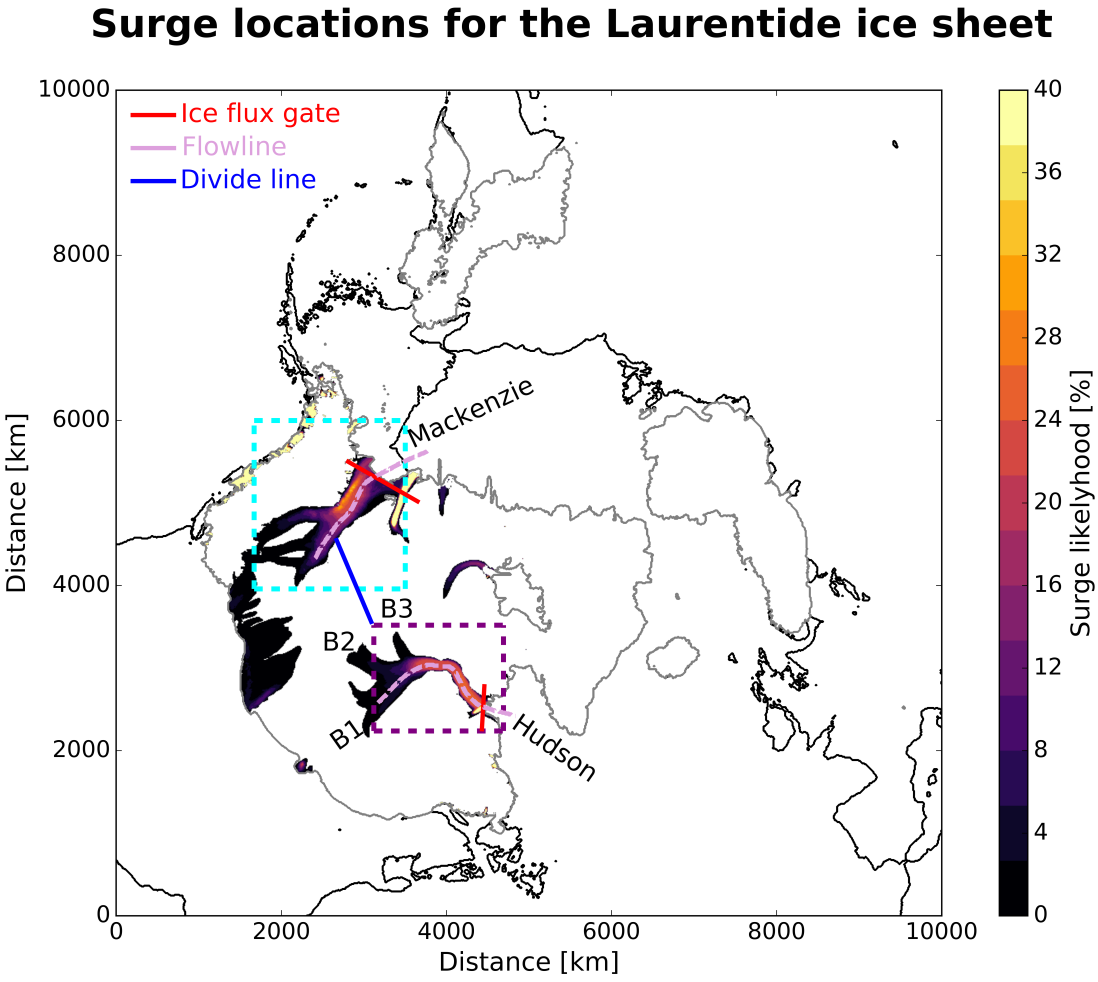

Figure 1. Overview of northern hemispheric ice-sheet model domain, highlighting surge regions from the Laurentide ice sheet. Surge likelyhood is calculated from the Ctrl simulation and is the percentage of time that the ice velocity in each cell exceeds 2,000 m yr^{-1}. Dashed cyan and purple boxes show areas used for ice volume calculations for Mackenzie and Hudson ice stream, respectively. Pink lines are flowline locations shown in Figs. 4 and 6. Red lines show flux gates across which ice flux for the respective ice stream is calculated. Solid blue line shows line approximately perpendicular to the drainage basin divide between Hudson and Mackenzie drainage basins. Labels B1, B2, and B3 depict different surge branches of the Hudson ice stream.

The current version of mPISM is based on PISM version 0.7.3. As in Ziemen et al. (2014), we modified the enthalpy advection to use the c-grid method that is also utilised for the mass advection. We also added the model fields and methods necessary for the coupling to the other model components. For the interpolation of the SSA velocities onto the c-grid, a weighted mean with 70% upwind and 30% downwind velocity is used. To improve the sliding behaviour necessary for the ice-sheet surges,

https://doi.org/10.5194/egusphere-2022-332
Preprint. Discussion started: 30 May 2022

we spread 50% of the basal heating effect from the sliding in each cell over the four neighbour cells. This leads to a better surge propagation. Following Calov et al. (2002) and Ziemen et al. (2019), basal sliding is discouraged in regions, where the sediment thickness map of Laske and Masters (1997) is less than 0.2 m.

At the base of the ice sheet, where ice is in contact with the subglacial topography, we apply a nonlinear Weertman-type friction law that links the basal shear stress $\boldsymbol{\tau}_b$ to the basal sliding velocity $\boldsymbol{u}_b$ of the form:

$$\boldsymbol{\tau}_b = -\tau_c \frac{\boldsymbol{u}_b}{u_0^q |\boldsymbol{u}_b|^{1-q}}. \tag{1}$$

where q is the basal sliding coefficient - set to 0.25 in all simulations, τ_c is the yield stress determined through the Mohr-Coulomb failure criterion, and u_0 is the threshold velocity at which the basal shear stress has the same magnitude as τ_c. We set u_0 to 70 m/yr for all simulations. If not stated otherwise, we apply a time and space invariant geothermal heat flux of 42 mW m^{-2}.

The initial state of our mPISM-VILMA simulations was taken at 36 ka from an MIS3 simulation with the Max Planck Institute for Meteorology ESM (MPI-ESM) asynchronously coupled to mPISM and VILMA. The MPI-ESM model system was adapted for long-term simulations in comparison to the version presented in Mauritsen et al. (2019) and accounts for changes in the land-sea mask, ocean bathymetrie (Meccia and Mikolajewicz, 2018), and river directions (Riddick et al., 2018) induced by changes in the glacial configuration. A detailed description of the MPI-ESM setup without the interactive ice-sheet and solid-earth components can be found in Kapsch et al. (2021, 2022). For the MIS3 simulation, MPI-ESM was additionally coupled to the solid-earth model VILMA and to a bi-hemispheric setup of mPISM, employing a 10 km resolution in the Northern Hemisphere and a 15 km resolution in the Southern Hemisphere. The coupling between MPI-ESM and mPISM-VILMA was performed asynchronously with an acceleration factor of 10 for the MPI-ESM component.

In the present study, we use a northern hemispheric setup of mPISM (Fig. 1) with a horizontal mesh resolution of 10 km. The coupling of mPISM and VILMA is performed every 100 model years and includes the exchange of the ice thickness distribution and GIA between the two models. Since VILMA is a global model, it requires a global ice thickness distribution as input. As we focus on the Laurentide ice sheet, we keep the ice thickness distribution of all other ice sheets constant through time.

2.2 Generation of idealised climate forcing

In order to investigate the effect of different forcing frequencies on the surge cycle, a cyclic forcing with favourable signal-to-noise ratio is desirable. However, because of non-linear processes involved, individual Heinrich-type ice sheet surges differ in their duration and ice-discharge evolution even under identical forcing. This introduces variability and results in an unfavourable signal-to-noise ratio. To mitigate this problem and permit simulations of arbitrary length, we generate an idealised forcing. For this, three different surge events are manually selected from the aforementioned MIS3 simulation with the asynchronously coupled MPI-ESM/mPISM/VILMA model system. We base the selection of characteristic surges on the Hudson ice stream, which is the most prominent surge region of the Laurentide ice sheet. The peak discharge of the three surges is manually matched and subsequently averaged (Fig. 2a). To create a single forcing for an individual surge cycle, we apply a si-

https://doi.org/10.5194/egusphere-2022-332
Preprint. Discussion started: 30 May 2022

nusoidal weight function to the mean forcing of the three events. The application of the weight function ensures that transitions between individual surge cycles are smooth (Fig. 2b). Each point in the final forcing function is a linear combination of two points from the mean forcing. For example, the center point of the final forcing is a result of a linear combination of weights from the center point of the mean forcing and the outermost point of the mean forcing (red points in Fig. 2a). These points are then progressively moved closer together during which their weights become more similar until they are neighbouring points with effectively equal weights (brown box in Fig. 2a). This process is carried out separately for the increasing and decreasing branch of the forcing cycle. Fig. 2 presents an example of the forcing generation for a one-dimensional variable field. For two-dimensional forcing fields, the same process is applied for each individual grid point. This method provides a forcing with a periodicity of 6500 years that consists of the climate feedback signal of an ice-sheet surge event and can be repeated as many times as desired. We use this procedure for the atmospheric and ocean forcing. The atmospheric forcing consists of 3D ice surface temperature and 3D SMB fields that are interpolated onto the current ice sheet topography. Both variable fields are calculated from atmospheric fields of the MPI-ESM/mPISM/VILMA simulation using an Energy Balance Model (EBM, Kapsch et al., 2021). The ice surface temperature hereby corresponds to the temperature of the lowest layer in a snow model (Kapsch et al., 2021), restricting ice surface temperature to values below freezing. Ocean forcing contains ocean temperature and salinity fields extracted from the ocean component of the MPI-ESM/mPISM/VILMA system.

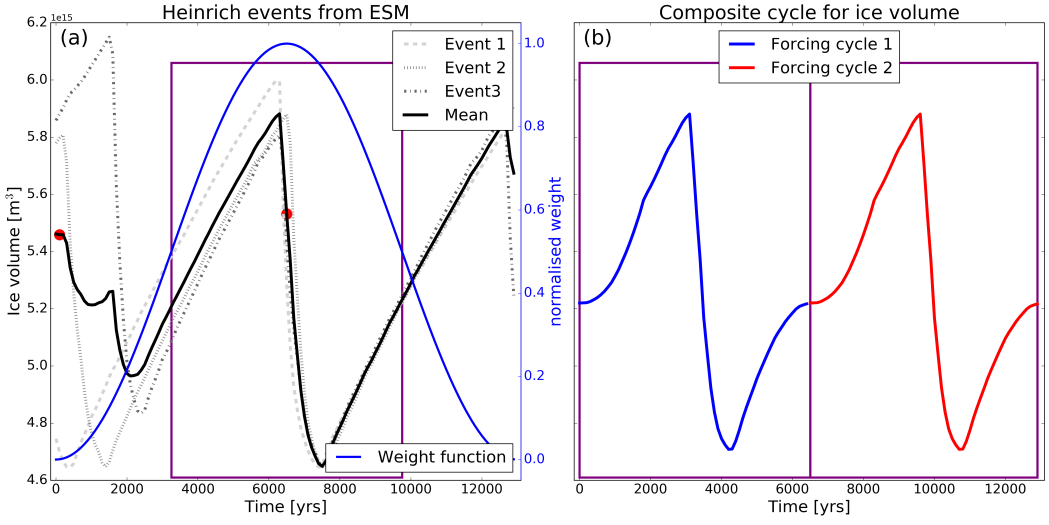

Figure 2. (a) Construction of composite forcing from individual ice-sheet surge events of Hudson ice stream from a MIS3 simulation with the MPI-ESM/mPISM/VILMA model system. Red dots indicate the start points for the application of the weighting function from which the final forcing is generated. (b) shows two cycles of ice volume changes from the composite forcing after the application of the weight function. There is a smooth transition from one forcing cycle to the next. Purple box in (a) corresponds to forcing cycles shown in (b) after the application of the weight function.

https://doi.org/10.5194/egusphere-2022-332
Preprint. Discussion started: 30 May 2022

Table 1. List of all perturbation experiments including type and magnitude of forcing. Abbreviations stand for control (Ctrl), geothermal heatflux (Geo), surface mass balance (Smb), ice surface temperature (St), sea level (Sl), ocean temperature (Ot), cyclic forcing (Cf), frozen (Froz), Hudson (Hud), and Mackenzie (Mac). The - and + signs represent negative and positive perturbations.

Experiment Name	Forcing type	Perturbation	Type of perturbation (magnitude)	Experiment type
Ctrl	Mean	Constant forcing	None	1
Geo+	Mean	Higher geothermal heatflux	Anomaly (+42 mW m^{-2})	1
Geo-	Mean	Lower geothermal heatflux	Anomaly (-42 mW m^{-2})	1
Smb+	Mean	SMB	Anomaly (+100 kg $m^{-2}yr^{-1}$)	1
Smb-	Mean	SMB	Anomaly (-100 kg $m^{-2}yr^{-1}$)	1
St-	Mean	Surface temperature	Anomaly (-5°C)	1
St+	Mean	Surface temperature	Anomaly (+5°C)	1
Sl-	Mean	Sea level	Anomaly (-10 m)	1
Sl+	Mean	Sea level	Anomaly (+10 m)	1
Ot+	Mean	Higher ocean temperature	Anomaly (+2°C)	1
Cf	Cyclic	Cyclic forcing	Frequency (6500 years)	2
CfSmb+	Cyclic	Higher SMB frequency	Frequency (factor 2 faster)	2
CfSmb-	Cyclic	Lower SMB frequency	Frequency (factor 2 slower)	2
CfGeo+	Cyclic	Higher GIA frequency	Frequency (factor 2 faster)	2
CfGeo-	Cyclic	Lower GIA frequency	Frequency (factor 2 slower)	2
CtrlFrozHud	Mean	Extreme negative geothermal heatflux	Anomaly (-1000 mW m^{-2})	3
CtrlFrozMac	Mean	Extreme negative geothermal heatflux	Anomaly (-1000 mW m^{-2})	3

3 Results and discussion

In the next sections, we will present and discuss the ensemble of ice sheet-solid earth simulations (Table 1). We use the control experiment Ctrl as baseline experiment. Ctrl uses a constant forcing, which is derived by taking the mean forcing of the cyclic forcing (Cf) outlined in Section 2.2. We use Ctrl to first provide an overview about the general surge behaviour of the Mackenzie and Hudson ice stream in our simulations. Subsequently, we use the Ctrl simulation to show that Hudson and Mackenzie ice stream exhibit a different surge initiation behaviour that is most likely caused by their distinct glaciological setting. We then explore the impact of the magnitude and variability of the boundary forcing on the surge cycle of the two ice streams. Finally, we investigate whether the surge behaviour of each individual ice stream is affected by surges of the other ice stream.

3.1 Surge behaviour of Hudson and Mackenzie ice streams in the control simulation

Both ice streams exhibit periodic high ice discharge events that we identify as ice-sheet surge events. The surges are a robust feature for most simulations presented here and have previously been shown for the Hudson ice stream in Ziemen et al. (2019).

https://doi.org/10.5194/egusphere-2022-332
Preprint. Discussion started: 30 May 2022

The surge frequency between the two regions differs significantly. The mean interval between ice-sheet surges is 4,900 years for the Mackenzie ice stream and 7,000 years for the Hudson ice stream (Fig. 3). This is in good agreement with proxy data for the Hudson ice stream which suggests a periodicity between 7,000-13,000 years (Heinrich, 1988). Overall, the Hudson ice stream exhibits larger peak discharge and the surges tend to be longer than for the Mackenzie ice stream. It is worth noting that the two surge regions appear to oscillate independently from each other. There is little variability for Hudson beyond the big surge events. In comparison, Mackenzie ice stream shows smaller intermittent increases in ice discharge between the major surge events (Fig. 3).

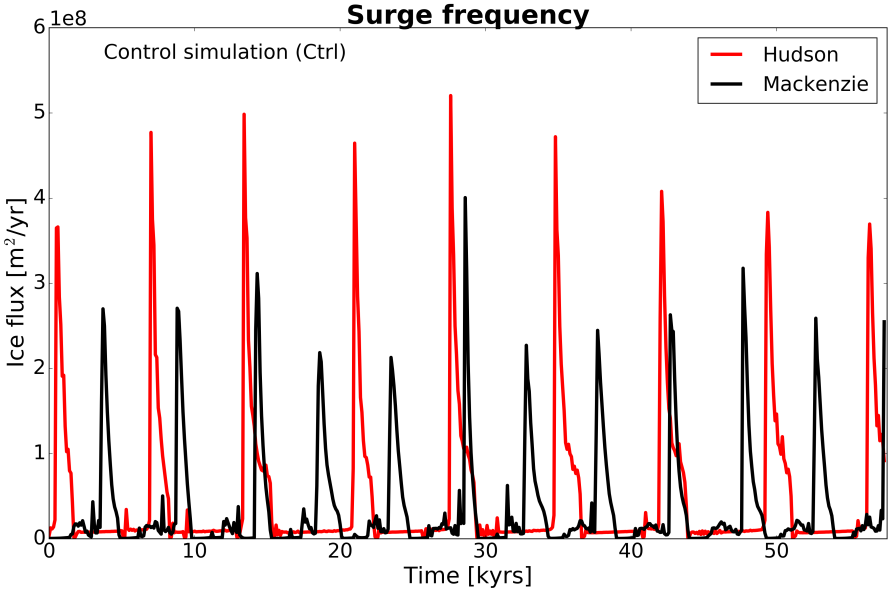

Figure 3. Timeseries of the ice flux through the flux gates presented in Fig. 1. Peak discharges define ice-sheet surge events.

3.2 Differences in surge mechanism between Mackenzie and Hudson ice stream

All ice-sheet surges in our model setup are the result of internal ice sheet oscillation that follow a binge-purge mechanism (MacAyeal, 1993). The basic surge mechanism is identical to the mechanism described in Calov et al. (2002). The surge sequence is described by three main stages: the quiescent phase, the pre-surge phase, and the surge phase. However, the initiation and propagation mechanisms differ, as the Mackenzie and Hudson ice stream differ in their glaciological setting. For the marine-terminating Hudson ice stream, only a small region close to the terminus is at pressure melting point (warm-based) during the quiescent phase, while the remaining parts further upstream are well below the pressure melting point (cold-based, Fig. 4b). As the ice sheet grows and enters the pre-surge phase, the warm-based region together with the availability of water at the base of the ice sheet expands upstream (Fig. 4e, f). When this region becomes large enough, the large ice velocity gradient at the bottom warm-cold boundary triggers an activation wave during which mechanical heat dissipation leads to an abrupt and

https://doi.org/10.5194/egusphere-2022-332
Preprint. Discussion started: 30 May 2022

widespread warming and lubricating of the ice stream. In about 100 years, this activation wave reaches the upper region of the drainage basin (Fig. 5). Almost all of the Hudson ice stream surges are characterised by contributions from three different surge branches (B1, B2, B3 in Fig. 1). The branches are almost exclusively activated in sequence, starting with branch B1 before
175 branches B2 and B3 surge (Fig. 5b). The next branch is activated when the previous branch ceases to exist. This is the case as soon as the active branch cannot draw down more ice to fuel the surge. The total surge phase lasts between 1,500-2,000 years before the advection of cold ice from upstream leads to a shutdown of the surge.

These results indicate that the surge initiation for the marine-terminating Hudson ice stream is driven from the ice-stream front

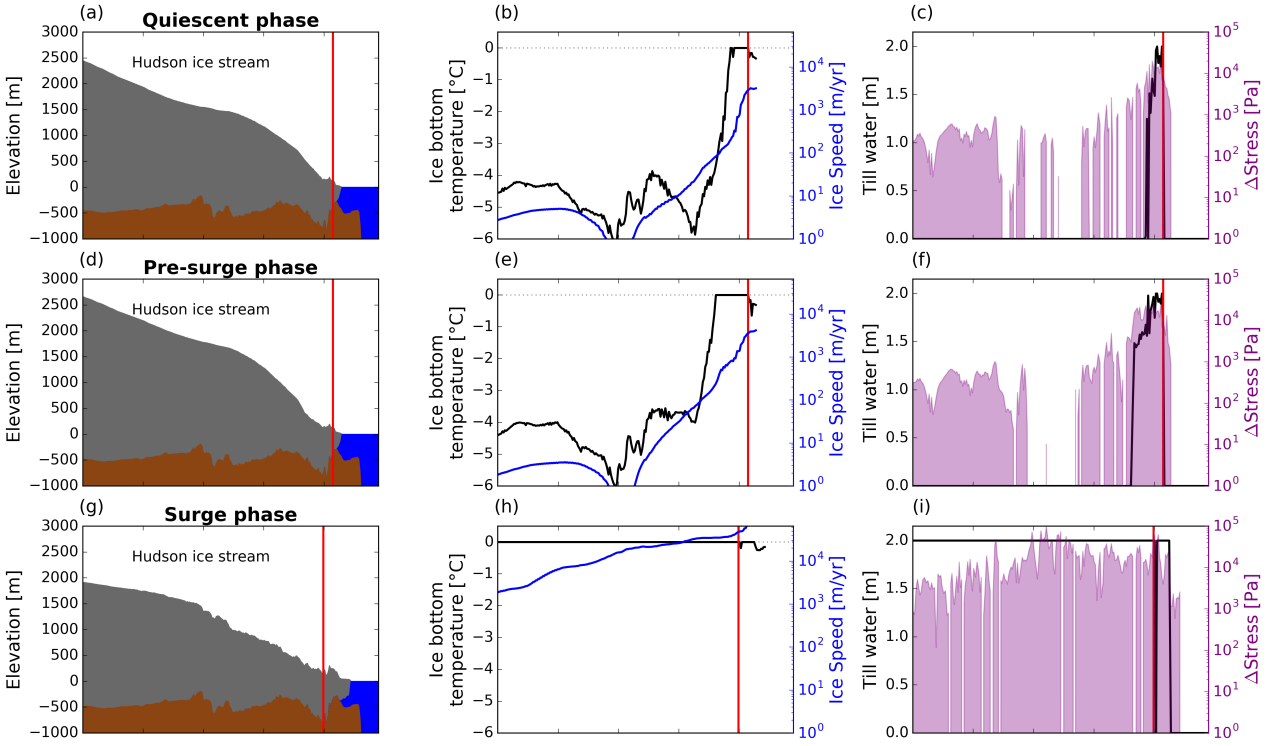

Figure 4. The three distinct phases during a canonical surge cycle for Hudson ice stream along the flowline in Fig. 1. Left panel shows ice sheet geometry. Middle panel shows pressure adjusted bottom temperature together with ice speed. Right panel shows thickness of basal water layer and ΔStress, where ΔStress = driving stress - basal shear stress. Red vertical line in approximates grounding-line position.

and propagates upstream. This is not the case for the land-terminating Mackenzie ice stream, for which the surge is initiated
180 from the upper reaches and propagates downstream. This difference in surge initiation is in agreement with observations from present-day land and marine-terminating glaciers in Svalbard (e.g. Sevestre et al., 2018). The terminus of the Mackenzie ice stream is well below the pressure melting point and therefore provides a barrier that has to be overcome for a surge event to take place. During the quiescent phase, the entire ice stream is frozen to its subglacial substrate, but the upper reaches of the ice stream are close to pressure melting point (Fig. 6b). This is likely a result of the generally warmer air temperatures for

https://doi.org/10.5194/egusphere-2022-332
Preprint. Discussion started: 30 May 2022

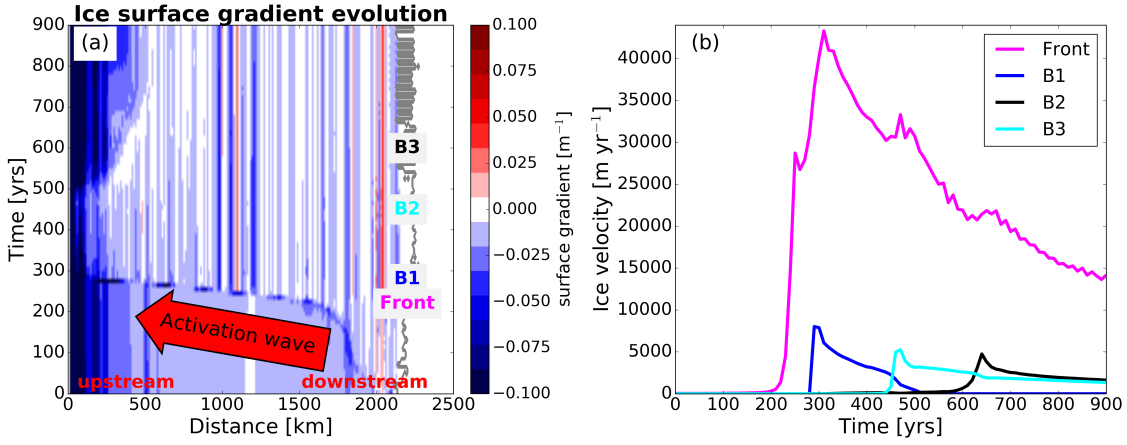

Figure 5. (a) Hovmoeller diagram of Hudson ice stream along the flowline (Fig. 1) during a surge event. The surface gradient captures the rapid upstream expansion of surge activation front. Grey line shows ice stream front. (b) shows activation of different surge branches of Hudson ice stream for the same surge event. Points for velocity sampling in (b) were manually selected. Labels in (a) refer to timing of surge activation of different branches (B1, B2, and B3) shown in (b).

this region caused by the lee effect of the Cordilleran ice sheet. In the pre-surge phase, narrow regions within the ice stream cause small-scale accelerations and advances of the ice sheet (Fig. 6d, e). However, as the ice stream is not preconditioned to surge yet, these accelerations are short-lived. Only when a large enough portion of the upstream part of the ice stream reaches the pressure melting point and the base of the ice sheet is lubricated a full surge develops. The surges are shorter (1,000-1,500 years) as compared to the Hudson ice stream (1,500-2,000 years). The shutdown of the surge follows the same pattern as for the Hudson ice stream. The absence of a well defined subglacial trough in the Mackenzie drainage basin results in more variable locations of the Heinrich-type ice sheet surges, a behaviour that is also supported by reconstructions of Mackenzie ice stream locations from proxy data (Margold et al., 2014). This underlines that the glaciological as well as the climatic setting alter the surge initiation process even though the governing surge mechanism for both ice streams is identical.

3.3 Sensitivity of surge cycle to anomaly forcing

In the following, we investigate which boundary forcing has the largest impact on the surge cycle. We test responses to perturbations of the SMB, ice surface temperature, geothermal heatflux, sea level, and ocean temperature. For all but the ocean temperature forcing, a positive and negative anomaly experiment is performed (Table 1). We compare the perturbations experiments to Ctrl.

In the positive (Smb+) and negative (Smb-) SMB experiments, the SMB is varied by ± 100 kg m^{-2} yr^{-1}. This corresponds to a perturbation that is $\sim$3 times and $\sim$6 times larger than the maximum SMB variation in Cf for the Mackenzie and Hudson drainage basins, respectively (Fig. A1). While this perturbation seems large, it falls into the range of what previous studies

https://doi.org/10.5194/egusphere-2022-332
Preprint. Discussion started: 30 May 2022

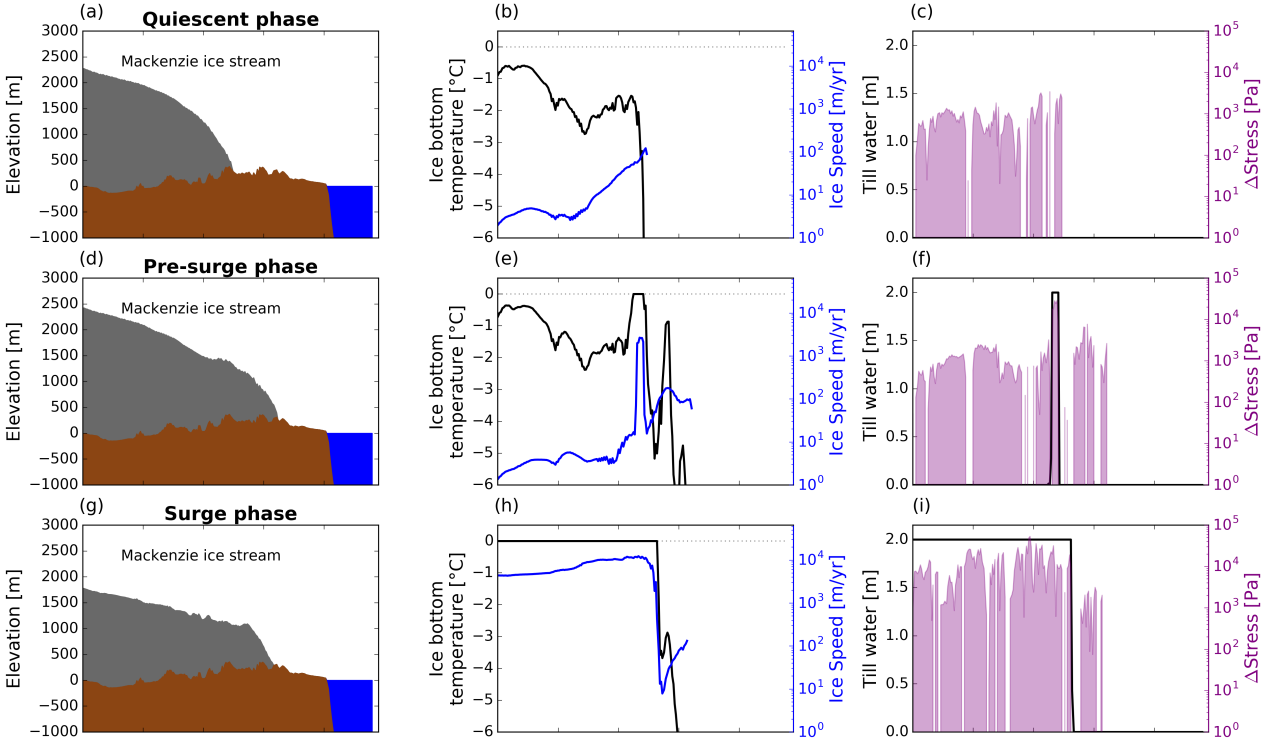

Figure 6. Similar to Fig. 4 but for Mackenzie ice stream.

have used (Calov et al., 2010; Bassis et al., 2017; Feldmann and Levermann, 2017).

The SMB perturbations significantly alter the surge cycle length. For the Hudson ice stream, the surge cycle length is reduced by ∼2,600 years for Smb+ to 4,400 years and lengthened by ∼5,600 years to 12,600 years for Smb-. A similar trend, albeit different in magnitude, is observed in Smb- for the Mackenzie ice stream, where the surge cycle length increases by ∼2,800 years to 7,600 years (Fig. 7a, b). For Smb+, the ice-sheet oscillations in the Mackenzie region cease to exist and turn this region into a persistent ice stream. For the Hudson ice stream, a shorter surge cycle length in Smb+ is associated with lower peak discharge values for each event, resulting in less (∼39%) ice volume discharge. In comparison, Smb- leads to a longer surge cycle with larger peak discharge values and an icrease in the discharged ice volume for each surge of ∼9%. The opposite is observed for Mackenzie ice stream, where a longer surge cycle in Smb- results in smaller peak discharge values and consequently a reduction in discharged ice volume of ∼28% per surge.

In the geothermal heatflux perturbation simulations (Geo+, Geo-), geothermal heatflux is varied by 42 mW m^{-2}, meaning geothermal heatflux ranges from 0-84 mW m^{-2} in our perturbation simulations. This choice remains well within the spatial variability range from geothermal heatflux maps of present-day North America (Lucazeau, 2019). Perturbations to the geothermal heatflux lead to smaller changes in the average surge cycle length than SMB perturbations for both regions. For Hudson ice stream, surge cycle length is shortened by ∼650 years to 6,350 years in Geo+ and lengthened by ∼1,300 to 8,300 years for

https://doi.org/10.5194/egusphere-2022-332
Preprint. Discussion started: 30 May 2022

Geo-. In Geo+, there is a change in the surge characteristic for Hudson ice stream with a shift towards double-peaked surges (B1 and B3 in Fig. 1). A continued addition of heat to the system turns the Hudson ice stream eventually into a persistent ice stream with smaller scale oscillations. The longer surge cycle length in Geo- results in larger peak discharge and discharged ice volume (∼15%) per surge event. For the Mackenzie area, the positive anomaly almost immediately turns this region into a persistent ice stream, while Geo- results in an extension of the surge cycle of ∼1,400 years to 6,300 years. Here, the longer surge cycle length is also associated with higher peak discharge values for individual surge events. However, the discharged ice volume for each surge event remains almost unchanged, but shows high variability from surge event to surge event (Fig. 8b)

In the ice surface temperature simulations (St-, St+), ice surface temperature is varied by 5°C. This is well below what proxy

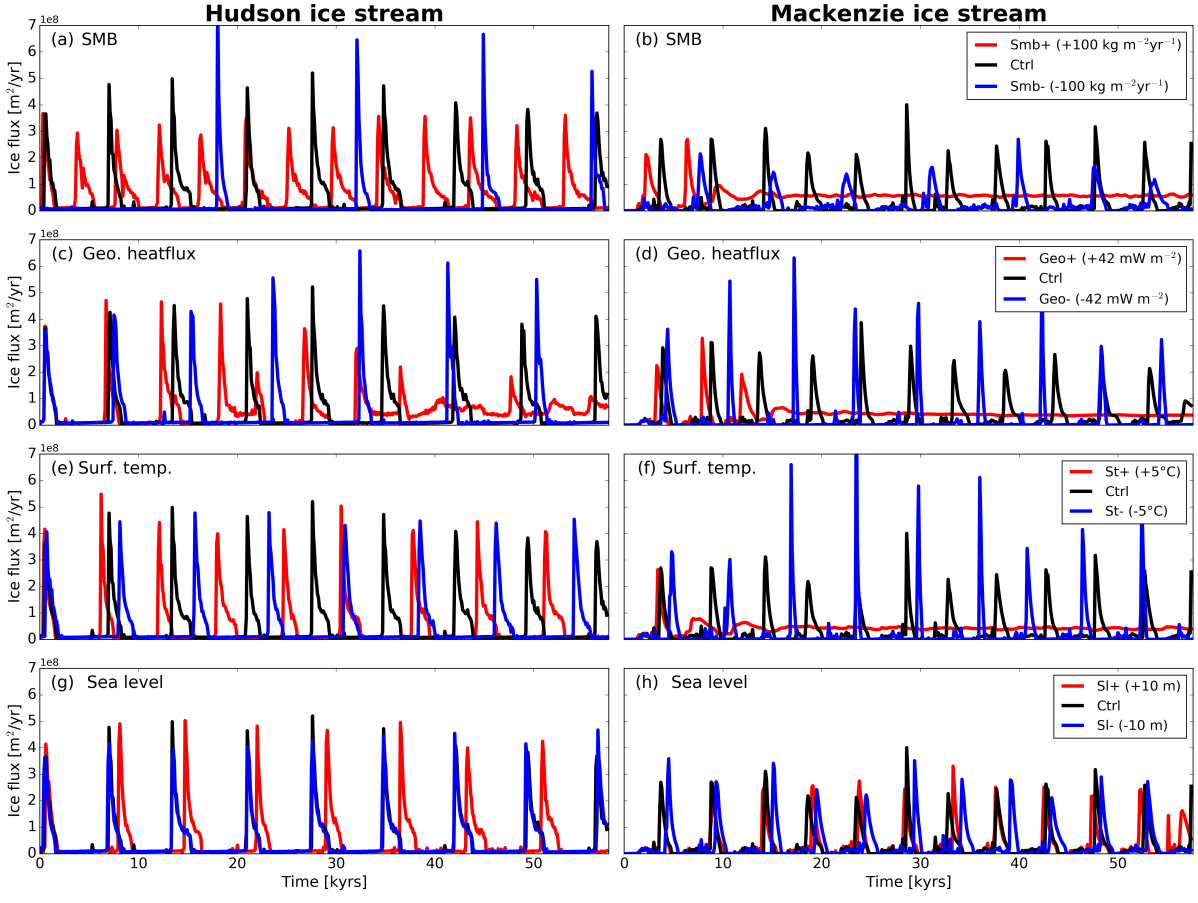

Figure 7. Similar to Fig. 3 but for Hudson (left) and Mackenzie (right) ice stream separately. The panels show response to (a,b) SMB, (c,d) geothermal heatflux, (e,f) ice surface temperature, and (g,h) sea level perturbations.

data suggest as temperature variations during a DO cycle (e.g. Kindler et al., 2014). The mean response to ice surface temperature perturbations is similar in magnitude to geothermal heatflux perturbations. For the Hudson ice stream, St+ results in a decrease of the surge cycle length of ∼600 years to 6,400 years. The surge cycle length is extended by the same amount in

https://doi.org/10.5194/egusphere-2022-332
Preprint. Discussion started: 30 May 2022

St-, leading to a surge cycle length of 7,600 years. The Mackenzie ice stream again turns into a persistent ice stream for St+, while St- results in an increase in surge cycle length of ∼1,400 years to 6,300 years, more than twice as large as the Hudson ice stream response (Fig. 7e, f). Large variations in peak discharge for the Mackenzie region are evident in St-, with large peak discharge events occuring more frequent. The higher peak discharge values are associated with a mean increase in discharged ice volume of ∼33% for each event. A similar correlation between changes in ice surface temperature and surge cycle length was found for individual models in ISMIP HEINO, but this correlation was not robust across all participating models (Calov et al., 2010).

In the sea level simulations (Sl-, Sl+), sea level is changed by 10 m. This is within the range of sea-level rise estimates for Heinrich-type ice sheet surges inferred from proxy data (e.g. Hemming, 2004) and is ∼8% of the sea-level change from the Last Glacial Maximum to present-day (Lambeck et al., 2014). Overall, sea-level perturbations have very little bearing on the surge cycle length (Fig. 7g, h). For Hudson ice stream, Sl- shows identical surge timing and magnitude as Ctrl. For Sl+, the surge interval is slightly lenghtened over the first three surge cycles before the system reaches a new equilibrium and oscillates at the same frequency as Ctrl, but surges are shifted by about 800 years (Fig. 7g). Peak discharge and discharged ice volume per surge remain practically unchanged in comparison to Ctrl. For Mackenzie ice stream, Sl- and Sl+ show very similar surge behaviour to Ctrl (Fig. 7h). This is expected as Mackenzie ice stream is land-terminating and therefore should be unaffected by changes in sea level. Mackenzie shows no change in surge cycle length, peak discharge, and discharged ice volume per surge event. However, the timing of the surges in Sl- and Sl+ differs slightly in comparison to Ctrl (Fig. 7h). We attribute these small changes to the high sensitivity of the Mackenzie ice stream to any system perturbations and its more variable surge behaviour in the absence of a well-defined subglacial trough.

In an additional simulation (Oc+), we also investigate the effect of warmer ocean temperatures for the marine-terminating Hudson ice stream. For this, the ocean temperature is increased by 2°C in the Oc+ simulation. However, Hudson ice stream only forms small floating ice tongues in our simulations. As a consequence, there is no change in surge cycle length for the Hudson ice stream to increased ocean temperatures (Fig. A2).

Of the five different boundary forcings, surge cycle length is most sensitive to changes in SMB. Ice surface temperature and geothermal heatflux also affect the surge cycle length but to a smaller extent. However, there are differences in the response of the two surge regions. St- shows that Mackenzie ice stream is more sensitive to changes in ice surface temperature than the Hudson ice stream, while Hudson ice stream responds more sensitive to changes in SMB (Fig. 8). We attribute these differences to differences in their respective climate settings. The Hudson ice stream area is characterised by ∼8-10 °C colder ice surface temperatures. The colder temperatures place the Hudson ice stream in a SMB regime that is dominated by accumulation with no ablation area (Fig. A1). This system reacts more sensitive to changes in SMB than an ice stream where the lower reaches experience significant amounts of ablation, as is the case for the Mackenzie ice stream. Due to very negative (<-500 kg m^{-2} yr^{-1}) ablation values for the Mackenzie region, the applied perturbations (±100 kg m^{-2} yr^{-1}) are relatively small in comparison to the Hudson ice stream, resulting in smaller changes to the surge cycle length.

The perturbation experiments highlight that the parameter space, under which ice-sheet oscillations are possible, is different for Mackenzie and Hudson ice stream. While Hudson ice stream only shows non-oscillatory behaviour in one of the perturbation

https://doi.org/10.5194/egusphere-2022-332
Preprint. Discussion started: 30 May 2022

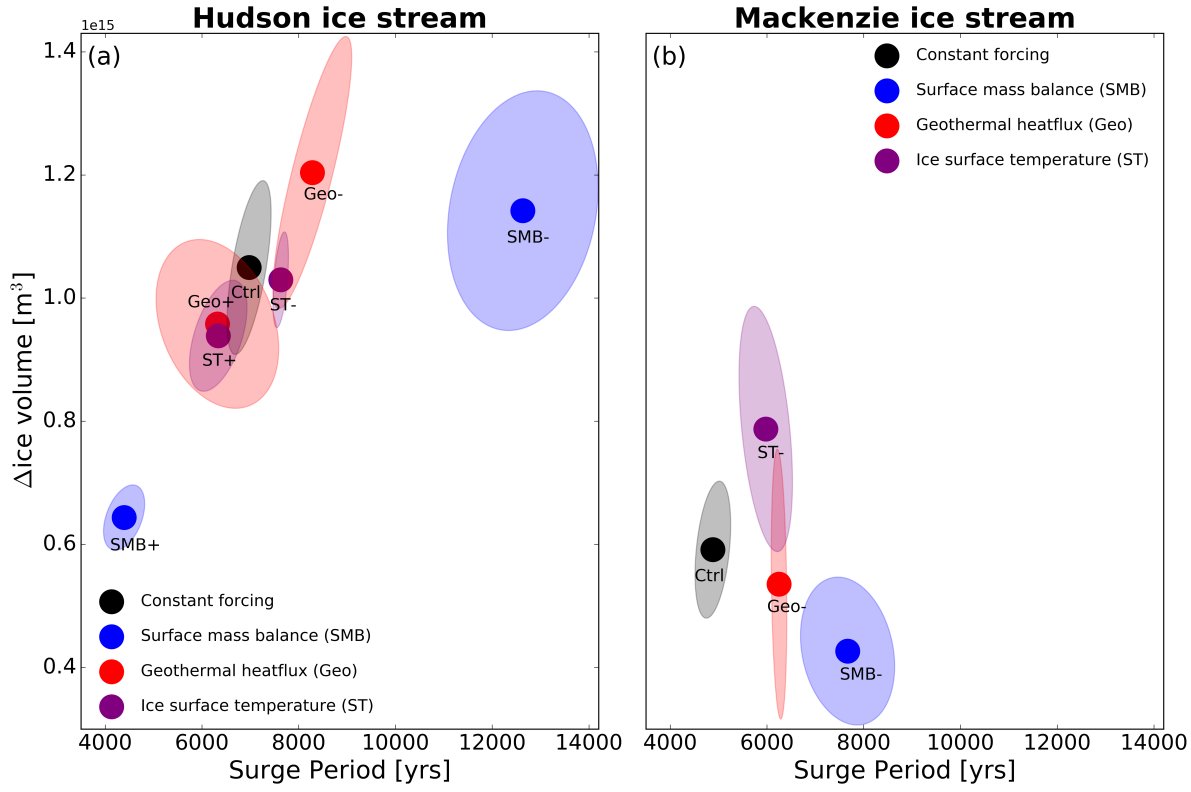

Figure 8. Ice volume change over surge period for (a) Hudson ice stream and (b) Mackenzie ice stream. Ice volume change is computed by taking the difference between maximum and minimum ice volume across each surge cycle. Ellipses show ±1 standard deviation. Sea level perturbations are omitted because they plot on top of Ctrl experiment for both regions. Positive perturbation simulations are missing in (b) because of an insufficient number of surges in these simulations due to the transition to a persistent ice stream.

simulations, Mackenzie ice stream enters the regime of persistent ice streaming for almost all positive perturbation simulations. We attribute this enhanced sensitivity of Mackenzie ice stream to the warmer climate conditions in this region, which is close to the climatic threshold that still supports ice-sheet surges. This is corroborated by the observation that the distribution of present-day surging glaciers also appears geographically bounded by key climatic parameters such as surface temperature and precipitation (Sevestre and Benn, 2015). The consequences of a regime shift from oscillations to a persistent ice stream are significant in terms of ice volume and associated sea-level rise over longer time scales (∼10,000 years). In the case of Hudson ice stream, such a regime shift results in a volume loss of 26% over the entire simulation length in comparison to the constant baseline simulation (Ctrl), adding up to a total of 3.3 m sea-level equivalent (Fig. 9a). For Mackenzie ice stream, the ice volume response is faster but smaller, primarily because its drainage basin is smaller in size and stores less ice. However, the increase in global sea level due to a regime shift of the Mackenzie ice stream still amounts to up to 1.8 m (Fig. 9b).

The applied perturbations in the experiments are below the estimated changes that occurred during the transition from the

https://doi.org/10.5194/egusphere-2022-332
Preprint. Discussion started: 30 May 2022

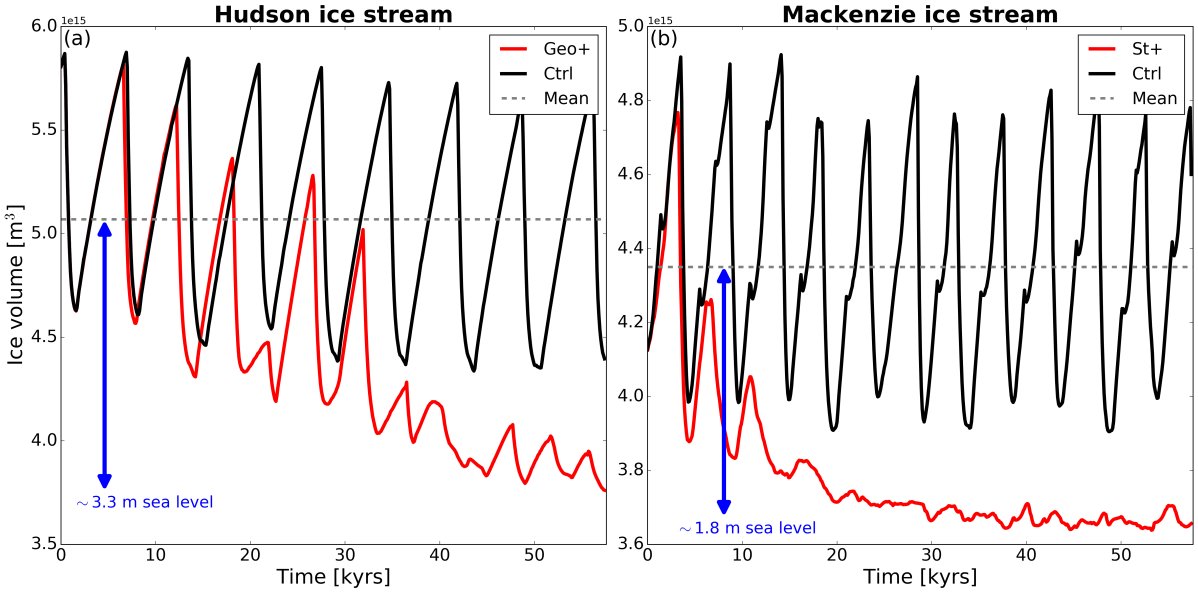

Figure 9. Comparison of ice volume evolution between oscillatory and persistent ice stream regime for the (a) Hudson and (b) Mackenzie ice stream.

Last Glacial Maximum to present-day. This indicates that the sensitivities presented in this study may have important ramifications for the progression of the last deglaciation. As Mackenzie ice stream is more sensitive to any climate warming signal than Hudson ice stream, it is more suceptible to have undergone the dynamical switch from an oscillatory system to a steady streaming system during the last deglaciation. Because of this enhanced sensitivity, we argue that it is also likely that this transition occurred in the earlier phase of the last deglaciation, potentially contributing to prominent abrupt climate change events of the last deglaciation such as Meltwater Pulse 1A (14.5 ka, Weaver et al. (2003)) or the onset of the Younger Dryas cold period. A previous study already indicated the potential contribution of Mackenzie ice stream to the onset of the Younger Dryas (Tarasov and Peltier, 2005). Possible consequences of such a dynamical switch go beyond the freshwater release into the ocean and sea-level response. A continuous loss of ice results in a lowering of the surface topography, potentially affecting the timing of the separation of the Laurentide and Cordilleran ice sheets, as well as changes in river directions, which can result in a redistribution of meltwater from the Laurentide ice sheet (Kapsch et al., 2022).

3.4 Sensitivity of the surge cycle to forcing frequency

We have investigated the surge cycle response to time invariant anomaly perturbations. Here, we study the effect of different forcing frequencies on the surge cycle. The cyclic forcing contains the climate feedback signal of the atmosphere and ocean component of the MPI-ESM/mPISM/VILMA model system during a surge event from the MIS3 period. The main objective is to investigate if this type of forcing is able to influence the timing of ice-sheet surges. For this, we performed a simulation with

https://doi.org/10.5194/egusphere-2022-332
Preprint. Discussion started: 30 May 2022

the cyclic forcing derived in Section 2.2 (Cf). We also performed additional simulations in which the frequency of the SMB was increased by a factor of two (Cfsmb+) or decreased by a factor of two (Cfsmb-). A similar kind of frequency perturbation was performed for the response of the glacial isostatic adjustment (GIA, Cfgeo+, Cfgeo-). In these simulations, mPISM was run without VILMA and the GIA forcing fields from Cf were either contracted or stretched by a factor of two.

First, we compare Cf with Ctrl. Cf has a forcing frequency of 6,500 years, while Ctrl has time constant forcing. In comparison to the anomaly perturbation simulations, the different forcing frequencies have very little effect on the surge cycle length. For Hudson ice stream, the surges are almost identical between the simulations. More variability is evident for the Mackenzie ice stream, but no clear trend emerges. That Mackenzie ice stream responds more sensitive to system perturbations is in accordance with the findings from the anomaly perturbation experiments. The cyclic climate forcing does not determine when surges occur in our simulations. This is evident because surges do not occur, when the climate forcing suggests that a surge should occur (Fig. 10, right panel).

The results are similar for the simulations in which only the frequency of the SMB or GIA forcing is varied. Differences are very small for the Hudson ice stream, regardless of the parameter that is being varied. Again, there is more variability in the response of Mackenzie ice stream, but there is no clear trend towards shorter surge cycles for a higher frequency forcing (Fig. 10, right panel). A potential reason for this increased variability is the absence of a well-defined subglacial trough in the Mackenzie region of the ice sheet.

Several studies have shown that ice-sheet surges can be phase locked (e.g. Calov et al., 2002; Kaspi et al., 2004; Mann et al., 2021). Phase locking refers to the observation that two weakly coupled autonomous oscillators with different natural frequencies can synchronise if they both are exposed to an external forcing that is strong enough to overcome the natural frequency of the two oscillators (Kaspi et al., 2004). In the present case, the two oscillators are the ice sheets and the climate system coupled through the boundary forcing. Phase locking has been used to explain the occurrence of ice-sheet surges during cold stadials of DO cycles, suggesting that a common climate trigger is determining the timing of ice-sheet surges (Kaspi et al., 2004; Mann et al., 2021). In our simulations, we do not observe a phase locking between the boundary forcing and surge activity, regardless of the parameter and forcing frequency (Fig. 10). Instead, both surge regions seem to be unaffected by the boundary forcing and continue oscillating at their natural frequency. This indicates that the climate signal present in the cyclic forcing from the MIS3 simulation is insufficient to cause phase locking. A potential explanation for the lack of phase locking is the inability of the ESM, from which the climate forcing for the presented simulations was taken, to produce DO-like climate oscillations. This means that shorter frequency oscillations like the 1,500 year long DO cycle are not included. It also suggests that the forcing magnitude is most likely underestimated because it only consists of the climate feedback signal induced by ice-sheet surges, but lacks the component of the DO events.

3.5 Telecommunication between surge regions

Phase locking has also been used to explain synchronised ice-sheet surges either from different locations of the Laurentide ice sheet or from different northern hemispheric ice sheets (Calov et al., 2002; Kaspi et al., 2004). In this section, we investigate how strong the coupling between the two surge regions is and how large of an effect surges of Mackenzie ice stream have

https://doi.org/10.5194/egusphere-2022-332
Preprint. Discussion started: 30 May 2022

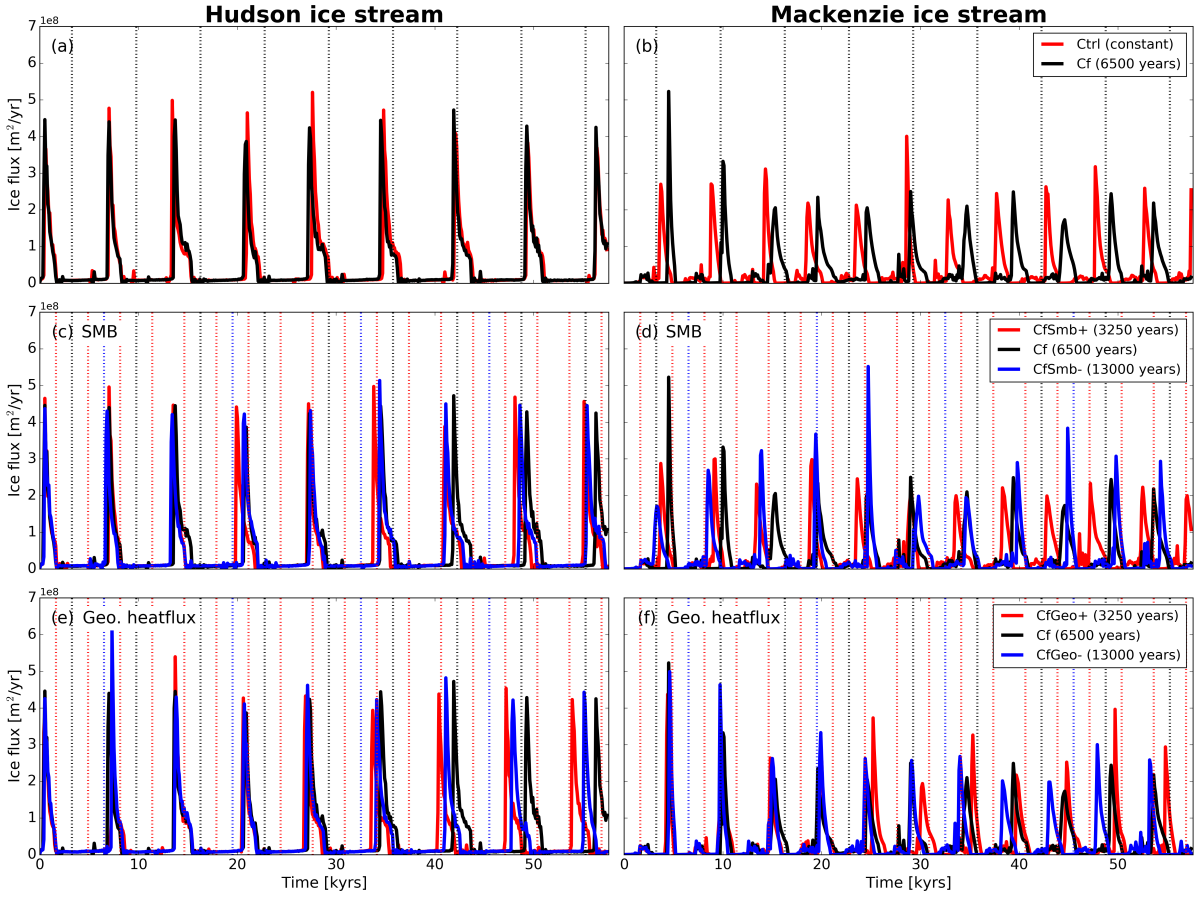

Figure 10. Similar to Fig. 3 but for Hudson (left) and Mackenzie (right) ice stream. The panel show response to (a,b) constant and cyclic forcing, (c,d) different SMB forcing frequencies, and (e,f) different glacial isostatic adjustment frequencies. The dashed vertical lines indicate when surge should occur according to the derived forcing. Numbers in parentheses in the legends indicate forcing frequency.

on surge characteristics of the Hudson ice stream and vice versa. To do this, we perform additional simulations in which we use constant boundary forcing similar to Ctrl, but artificially suppress surging in one of the two surge regions. Surges are suppressed by applying a negative geothermal heatflux that keeps the ice-sheet base well below pressure melting point (CtrlFrozHud, CtrlFrozMac).

The surge regions are dynamically connected because they share a common ice divide. The position of the divide marks the highest point of the Laurentide ice sheet and also marks the boundary of the drainage basins of Mackenzie and Hudson ice stream. In Ctrl, the divide migrates by ∼200 km over a time span of ∼1,500 years between surge events. During an ice sheet surge, the dynamic thinning that accompanies the increase in ice discharge results in a migration of the ice divide and a growing of the drainage basin area. On a much smaller scale, this has also been modelled for Antarctic ice rises (e.g. Schannwell et al., 2019). However, the long-time mean position of the divide remains unchanged (Fig. 11). This means that the average

https://doi.org/10.5194/egusphere-2022-332
Preprint. Discussion started: 30 May 2022

drainage basin area of the surge regions does not change and, hence, changes in surge characteristics are not to be expected. In CtrlFrozHud and CtrlFrozMac the ice stream that remains active experiences a lasting increase in drainage basin size. In both simulations, the divide migrates by ∼400 km into the drainage basin of the inactive region. The larger drainage basin offers the potential for a change in surge characteristics because it allows for more accessible ice volume that potentially could be mobilised during a surge event. This leads to a change in surge behaviour for the Hudson ice stream, but there is little change for the Mackenzie ice stream, despite a similar increase in drainage basin area. The reason for the different response is that the added drainage basin area is never activated in subsequent surges of the Mackenzie ice stream. This is due to the fact that the added drainage basin area for Mackenzie ice stream remains well below pressure melting point during the subsequent surge events. In contrast, the Hudson ice stream surges now propagate much further upstream, which switches the single-peaked surge regime to a double-peaked surge regime (Fig. 11a), also observed in the Geo+ simulation. The double-peaked surges are characterised by surges from two different branches of the ice stream (see B1 and B3 in Fig. 1). In between the ice discharge maxima, elevated ice velocities and ice discharge are maintained. Only when the second branch starts to surge does the other ice stream cease to exist. These results show that the drainage basin size is an indicator for the potential magnitude of ice discharge, but only under the assumption that the added ice volume is actually activated during surges.

The position of the main ice divide of the Laurentide ice sheet has also implications for the atmospheric circulation, which is not considered in our model system. Because it marks the highest point of the ice sheet, it provides a barrier for atmospheric flow. It has been shown in previous studies using ice-sheet reconstructions that different ice sheet heights strongly affect the climate response (e.g. Ullman et al., 2014; Bakker et al., 2020; Kapsch et al., 2022). Hence, it is reasonable to conclude that ice divide migration of several hundred kilometer east or west is likely to affect the climate response.

As suggested by some proxy data (e.g. Grousset et al., 2000) and simulated in simple box models (Kaspi et al., 2004), synchronisation of surge events from different ice sheets or different regions of the same ice sheet can occur through phase locking. With our standard setup employed here, synchronised surges cannot be reproduced through phase locking. However, as both surge regions are sensitive to different boundary forcings, it is possible to simulate synchronised surge events with our model setup under certain climate conditions. In Geo- for Mackenzie ice stream and St+ for Hudson ice stream, the surge cycle length is almost identical (Fig. 12a). The perturbation to the climate forcing to achieve this synchronicity are within a realistic range, considering the uncertainties of certain parameters (e.g. geothermal heatflux) in the model setup. The scenario of synchronised surges from the Laurentide ice sheet has important implications for the global climate response as more meltwater is added simultaneously at multiple geographic locations to the ocean. The importance of the amount of added freshwater and the location of the freshwater input for the global ocean response has been highlighted by a variety of freshwater hosing experiments (e.g. Maier-Reimer and Mikolajewicz, 1989; Schiller et al., 1997; Stouffer et al., 2006; Smith and Gregory, 2009; Lohmann et al., 2020).

https://doi.org/10.5194/egusphere-2022-332
Preprint. Discussion started: 30 May 2022

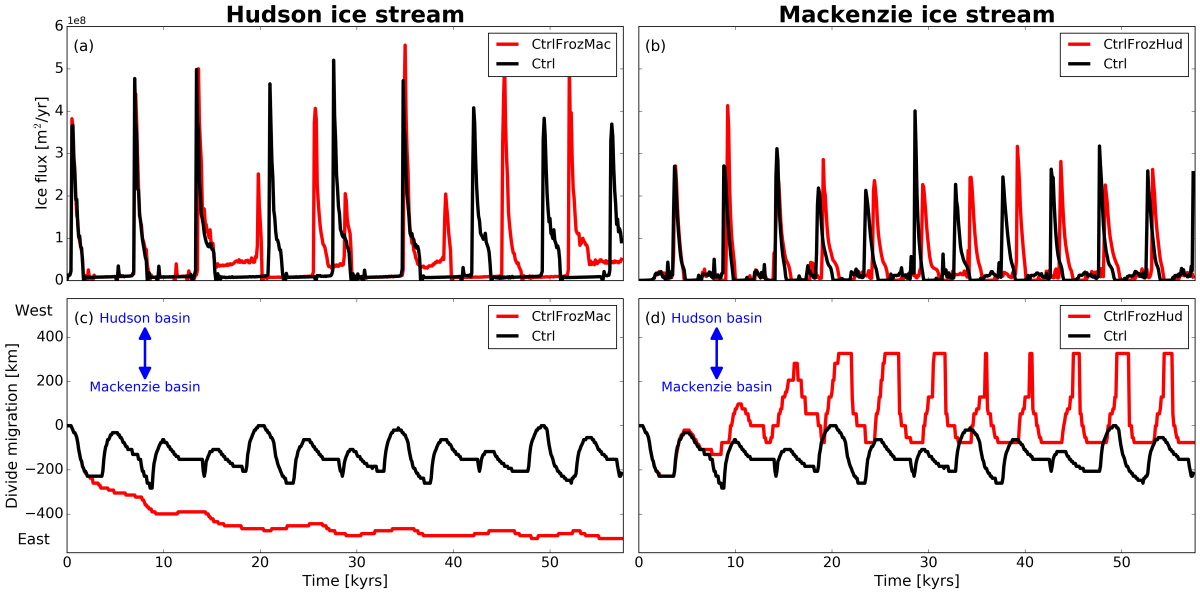

Figure 11. Differences induced by artificially suppressing surge events in one of the surge regions. Upper panel (a,b) shows timeseries of ice flux through the flux gates (Fig. 1). Lower panel (c,d) shows temporal evolution of ice divide position (Fig. 1).

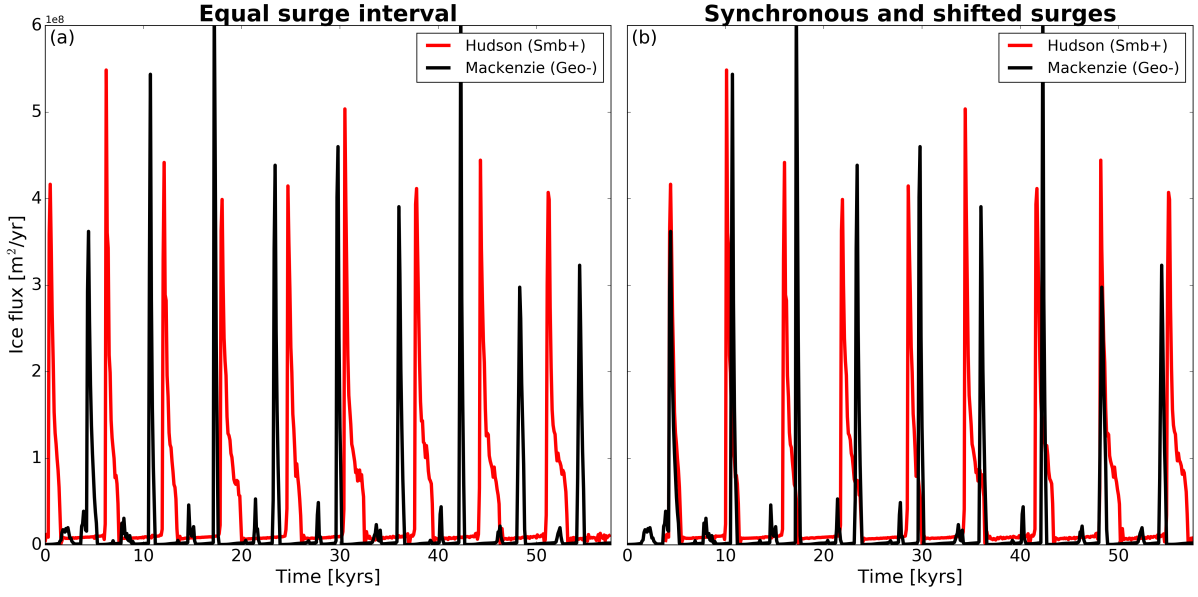

Figure 12. Timeseries of the ice flux through the flux gate (Fig. 1) for Hudson and Mackenzie ice stream showing (a) equal surge interval and (b) synchronous surges.

https://doi.org/10.5194/egusphere-2022-332
Preprint. Discussion started: 30 May 2022

4 Conclusions

Our simulations identify the SMB as the most important driver controlling the surge cycle length of Heinrich-type ice sheet surges (Fig. 8), confirming earlier findings from the ISMIP HEINO experiments with highly idealised geometries and simpler ice mechanical models (Calov et al., 2010). While geothermal heatflux and surface temperature also influence the surge cycle length, albeit to a smaller extent, ocean and sea-level forcing as well as different forcing frequencies play a negligible role. This is in contrast to findings from earlier studies (Calov et al., 2002; Alvarez-Solas et al., 2013; Bassis et al., 2017). The likely reasons for the insensitivity of Hudson ice stream to warmer ocean temperatures is that in our simulations Hudson ice stream never forms an extensive ice shelf that could provide a stabilising force. We also show that the modelled land and marine-terminating glaciers exhibit different surge initiation behaviour that is similar to the surge initiation behaviour from present-day land and marine-terminating glaciers in Svalbard (Sevestre et al., 2018). For the marine-terminating Hudson ice stream, which is in contact with warmer ocean water, the surge is initiated at the ice stream front and propagates upstream, while for the land-terminating Mackenzie ice stream surge initiation occurs further upstream and the wave propagates downstream. Both regions are affected by surges of the other region through the migration of the ice divide that their drainage basins share. However, the increase in drainage basin size only leads to a change in surge behaviour towards double-peaked events for the Hudson ice stream. Even though the peak ice discharge does not change, the length of the surge is extended, leading to a higher ice volume loss for each surge event. The surge behaviour remains unchanged for the Mackenzie ice stream because the additional available ice volume is not activated during the surges. Synchronised surges from the Mackenzie and Hudson ice stream cannot be modelled under the control boundary forcing, but are possible under certain boundary forcing combinations e.g. Smb+ for Hudson and Geo- for Mackenzie ice stream.

The simulations also highlight that Mackenzie ice stream is close to a parameter regime under which ice-sheet oscillations cannot be maintained. The dynamical switch from oscillations to persistent ice streaming can result in a volume loss of up to 15% and 26% in comparison to constant climate conditions for Mackenzie and Hudson ice stream, respectively. If both regions enter the ice streaming parameter space at a similar time, an additional 5.1 m of sea-level equivalent could be added to the global ocean. The extreme sensitivity of Mackenzie ice stream to any positive climate perturbation underlines the potential of Mackenzie ice stream to have contributed to prominent abrupt climate change events during glacial-interglacial transitions, such as the Younger Dryas cold period.

https://doi.org/10.5194/egusphere-2022-332
Preprint. Discussion started: 30 May 2022

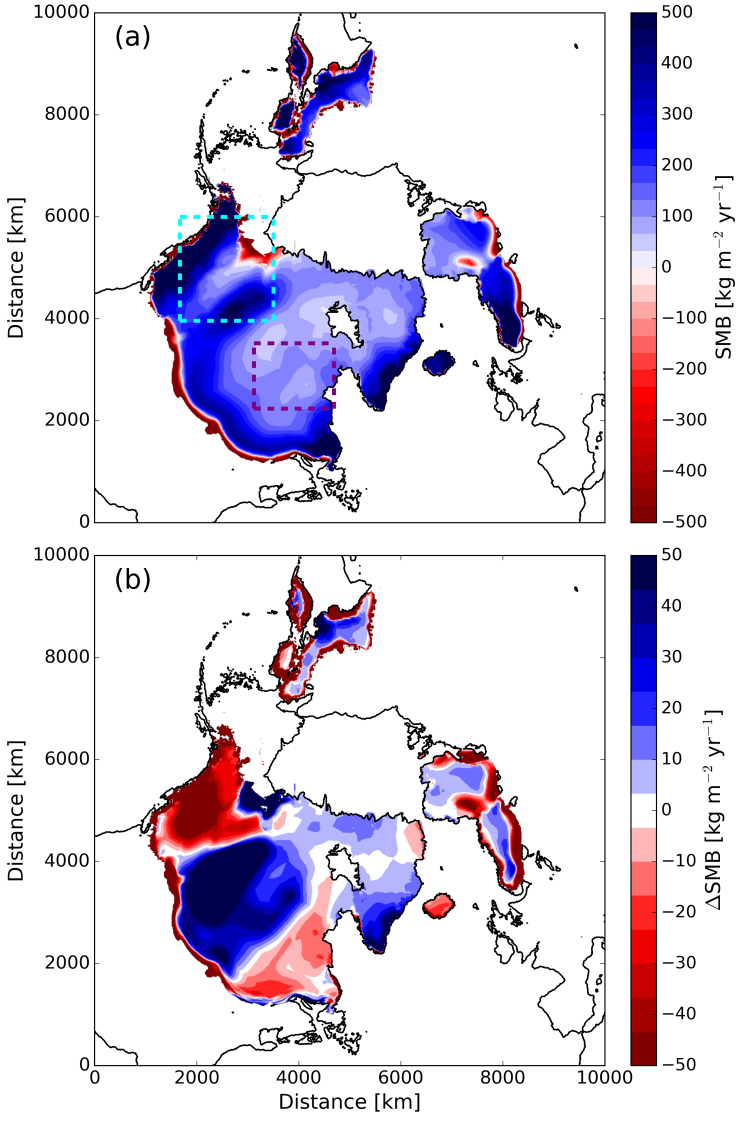

Figure A1. (a) Mean SMB field for one cycle of the idealised forcing. (b) Difference in SMB before and after a surge event for one cycle of the idealised forcing. Cyan and purple dashed boxes in (a) show Mackenzie and Hudson area respectively.

https://doi.org/10.5194/egusphere-2022-332
Preprint. Discussion started: 30 May 2022

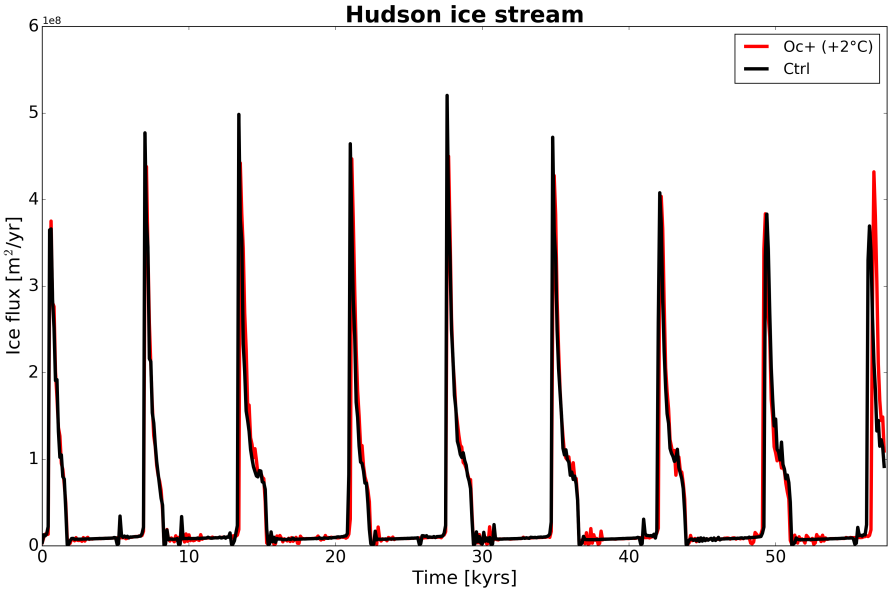

Figure A2. Timeseries of ice flux through the flux gate (Fig. 1) for ocean perturbation for Hudson ice stream.

Code and data availability. The PISM model code is publicly available through GitHub (https://github.com/pism/pism/, last access 01 April 2022). All scripts and required input data to reproduce all figures in the manuscript are available under the following link https://doi.org/10.5281/zenodo.6519774.

Author contributions. CS and UM conceived the study. FAZ developed the setup with input from MLK. CS performed the experiments. CS analysed the data. The manuscript was written by CS with input from all co-authors.

Competing interests. The authors declare that they have no conflict of interest.

Acknowledgements. C. Schannwell, M. Kapsch and U. Mikolajewicz were supported by the German Federal Ministry of Education and Research (BMBF) as a Research for Sustainability initiative (FONA) through the PalMod project under the grant numbers 01LP1915C, 01LP1502A, and 01LP1917B. This work used resources of the Deutsches Klimarechenzentrum (DKRZ) granted by its Scientific Steering Committee (WLA) under project ID ba0989. Development of PISM is supported by NSF grants PLR-1644277 and PLR-1914668 and NASA grants NNX17AG65G and 20-CRYO2020-0052. We thank Andreas Wernecke for comments which improved the manuscript.

https://doi.org/10.5194/egusphere-2022-332
Preprint. Discussion started: 30 May 2022

References

Álvarez-Solas, J., Montoya, M., Ritz, C., Ramstein, G., Charbit, S., Dumas, C., Nisancioglu, K., Dokken, T., and Ganopolski, A.: Heinrich event 1: an example of dynamical ice-sheet reaction to oceanic changes, Climate of the Past, 7, 1297–1306, https://doi.org/10.5194/cp-7-1297-2011, 2011.

Alvarez-Solas, J., Robinson, A., Montoya, M., and Ritz, C.: Iceberg discharges of the last glacial period driven by oceanic circulation changes, Proceedings of the National Academy of Sciences, 110, 16 350–16 354, https://doi.org/10.1073/pnas.1306622110, 2013.

Bakker, P., Rogozhina, I., Merkel, U., and Prange, M.: Hypersensitivity of glacial summer temperatures in Siberia, Climate of the Past, 16, 371–386, https://doi.org/10.5194/cp-16-371-2020, 2020.

Bassis, J. N., Petersen, S. V., and Cathles, L. M.: Heinrich events triggered by ocean forcing and modulated by isostatic adjustment, Nature, 542, 332–334, 2017.

Bond, G., Broecker, W., Johnsen, S., McManus, J., Labeyrie, L., Jouzel, J., and Bonani, G.: Correlations between climate records from North Atlantic sediments and Greenland ice, Nature, 365, 143–147, https://doi.org/10.1038/365143a0, 1993.

Broecker, W. S.: Massive iceberg discharges as triggers for global climate change, Nature, 372, 421–424, 1994.

Broecker, W. S., Kennett, J. P., Flower, B. P., Teller, J. T., Trumbore, S., Bonani, G., and Wolfli, W.: Routing of meltwater from the Laurentide Ice Sheet during the Younger Dryas cold episode, Nature, 341, 318–321, https://doi.org/10.1038/341318a0, 1989.

Calov, R., Ganopolski, A., Petoukhov, V., Claussen, M., and Greve, R.: Large-scale instabilities of the Laurentide ice sheet simulated in a fully coupled climate-system model, Geophysical Research Letters, 29, 69–1–69–4, https://doi.org/10.1029/2002gl016078, 2002.

Calov, R., Greve, R., Abe-Ouchi, A., Bueler, E., Huybrechts, P., Johnson, J. V., Pattyn, F., Pollard, D., Ritz, C., Saito, F., and Tarasov, L.: Results from the Ice-Sheet Model Intercomparison Project–Heinrich Event Intercomparison (ISMIP HEINO), Journal of Glaciology, 56, 371–383, https://doi.org/10.3189/002214310792447789, 2010.

Condron, A. and Winsor, P.: Meltwater routing and the Younger Dryas, Proceedings of the National Academy of Sciences, 109, 19 928–19 933, https://doi.org/10.1073/pnas.1207381109, 2012.

de Vernal, A., Hillaire-Marcel, C., Turon, J.-L., and Matthiessen, J.: Reconstruction of sea-surface temperature, salinity, and sea-ice cover in the northern North Atlantic during the last glacial maximum based on dinocyst assemblages, Canadian Journal of Earth Sciences, 37, 725–750, https://doi.org/10.1139/e99-091, 2000.

Feldmann, J. and Levermann, A.: From cyclic ice streaming to Heinrich-like events: the grow-and-surge instability in the Parallel Ice Sheet Model, The Cryosphere, 11, 1913–1932, https://doi.org/10.5194/tc-11-1913-2017, 2017.

Grousset, F. E., Pujol, C., Labeyrie, L., Auffret, G., and Boelaert, A.: Were the North Atlantic Heinrich events triggered by the behavior of the European ice sheets?, Geology, 28, 123–126, https://doi.org/10.1130/0091-7613(2000)28<123:WTNAHE>2.0.CO;2, 2000.

Heinrich, H.: Origin and Consequences of Cyclic Ice Rafting in the Northeast Atlantic Ocean During the Past 130,000 Years, Quaternary Research, 29, 142–152, https://doi.org/10.1016/0033-5894(88)90057-9, 1988.

Hemming, S. R.: Heinrich events: Massive late Pleistocene detritus layers of the North Atlantic and their global climate imprint, Reviews of Geophysics, 42, https://doi.org/10.1029/2003rg000128, 2004.

Holland, D. M. and Jenkins, A.: Modeling Thermodynamic Ice–Ocean Interactions at the Base of an Ice Shelf, Journal of Physical Oceanography, 29, 1787–1800, https://doi.org/10.1175/1520-0485(1999)029<1787:mtioia>2.0.co;2, 1999.

Hulbe, C. L., MacAyeal, D. R., Denton, G. H., Kleman, J., and Lowell, T. V.: Catastrophic ice shelf breakup as the source of Heinrich event icebergs, Paleoceanography, 19, n/a–n/a, https://doi.org/10.1029/2003pa000890, 2004.

https://doi.org/10.5194/egusphere-2022-332
Preprint. Discussion started: 30 May 2022

Kapsch, M.-L., Mikolajewicz, U., Ziemen, F. A., Rodehacke, C. B., and Schannwell, C.: Analysis of the surface mass balance for deglacial climate simulations, The Cryosphere, 15, 1131–1156, https://doi.org/10.5194/tc-15-1131-2021, 2021.

Kapsch, M.-L., Mikolajewicz, U., Ziemen, F., and Schannwell, C.: Ocean Response in Transient Simulations of the Last Deglaciation Dominated by Underlying Ice-Sheet Reconstruction and Method of Meltwater Distribution, Geophysical Research Letters, 49, https://doi.org/10.1029/2021gl096767, 2022.

Kaspi, Y., Sayag, R., and Tziperman, E.: A "triple sea-ice state" mechanism for the abrupt warming and synchronous ice sheet collapses during Heinrich events, Paleoceanography, 19, n/a–n/a, https://doi.org/10.1029/2004pa001009, 2004.

Kindler, P., Guillevic, M., Baumgartner, M., Schwander, J., Landais, A., and Leuenberger, M.: Temperature reconstruction from 10 to 120 kyr b2k from the NGRIP ice core, Climate of the Past, 10, 887–902, https://doi.org/10.5194/cp-10-887-2014, 2014.

Lambeck, K., Rouby, H., Purcell, A., Sun, Y., and Sambridge, M.: Sea level and global ice volumes from the Last Glacial Maximum to the Holocene, Proceedings of the National Academy of Sciences, 111, 15 296–15 303, https://doi.org/10.1073/pnas.1411762111, 2014.

Laske, G. and Masters, G.: A Global Digital Map of Sediment Thickness, EOS Trans. AGU, 78, 1997.

Lin, Y., Hibbert, F. D., Whitehouse, P. L., Woodroffe, S. A., Purcell, A., Shennan, I., and Bradley, S. L.: A reconciled solution of Meltwater Pulse 1A sources using sea-level fingerprinting, Nature Communications, 12, https://doi.org/10.1038/s41467-021-21990-y, 2021.

Lohmann, G., Butzin, M., Eissner, N., Shi, X., and Stepanek, C.: Abrupt Climate and Weather Changes Across Time Scales, Paleoceanography and Paleoclimatology, 35, e2019PA003 782, https://doi.org/https://doi.org/10.1029/2019PA003782, 2020.

Lucazeau, F.: Analysis and Mapping of an Updated Terrestrial Heat Flow Data Set, Geochemistry, Geophysics, Geosystems, 20, 4001–4024, https://doi.org/https://doi.org/10.1029/2019GC008389, 2019.

MacAyeal, D. R.: Binge/purge oscillations of the Laurentide Ice Sheet as a cause of the North Atlantic's Heinrich events, Paleoceanography, 8, 775–784, https://doi.org/10.1029/93PA02200, 1993.

Maier-Reimer, E. and Mikolajewicz, U.: Experiments with an OGCM on the Cause of the Younger Dryas, vol. no. 39 of *Max-Planck-Institut für Meteorologie report*, Max-Planck-Institut für Meteorologie, 1989.

Mann, L. E., Robel, A. A., and Meyer, C. R.: Synchronization of Heinrich and Dansgaard-Oeschger Events Through Ice-Ocean Interactions, Paleoceanography and Paleoclimatology, 36, e2021PA004 334, https://doi.org/https://doi.org/10.1029/2021PA004334, e2021PA004334 2021PA004334, 2021.

Marcott, S. A., Clark, P. U., Padman, L., Klinkhammer, G. P., Springer, S. R., Liu, Z., Otto-Bliesner, B. L., Carlson, A. E., Ungerer, A., Padman, J., He, F., Cheng, J., and Schmittner, A.: Ice-shelf collapse from subsurface warming as a trigger for Heinrich events, Proceedings of the National Academy of Sciences, 108, 13 415–13 419, https://doi.org/10.1073/pnas.1104772108, 2011.

Margold, M., Stokes, C. R., Clark, C. D., and Kleman, J.: Ice streams in the Laurentide Ice Sheet: a new mapping inventory, Journal of Maps, 11, 380–395, https://doi.org/10.1080/17445647.2014.912036, 2014.

Martinec, Z., Klemann, V., van der Wal, W., Riva, R. E. M., Spada, G., Sun, Y., Melini, D., Kachuck, S. B., Barletta, V., Simon, K., A, G., and James, T. S.: A benchmark study of numerical implementations of the sea level equation in GIA modelling, Geophysical Journal International, 215, 389–414, https://doi.org/10.1093/gji/ggy280, 2018.

Mauritsen, T., Bader, J., Becker, T., Behrens, J., Bittner, M., Brokopf, R., Brovkin, V., Claussen, M., Crueger, T., Esch, M., Fast, I., Fiedler, S., Fläschner, D., Gayler, V., Giorgetta, M., Goll, D. S., Haak, H., Hagemann, S., Hedemann, C., Hohenegger, C., Ilyina, T., Jahns, T., de-la Cuesta, D. J., Jungclaus, J., Kleinen, T., Kloster, S., Kracher, D., Kinne, S., Kleberg, D., Lasslop, G., Kornblueh, L., Marotzke, J., Matei, D., Meraner, K., Mikolajewicz, U., Modali, K., Möbis, B., Müller, W. A., Nabel, J. E. M. S., Nam, C. C. W., Notz, D., Nyawira, S.-S., Paulsen, H., Peters, K., Pincus, R., Pohlmann, H., Pongratz, J., Popp, M., Raddatz, T. J., Rast, S., Redler, R., Reick, C. H., Rohrschneider,

https://doi.org/10.5194/egusphere-2022-332
Preprint. Discussion started: 30 May 2022

T., Schemann, V., Schmidt, H., Schnur, R., Schulzweida, U., Six, K. D., Stein, L., Stemmler, I., Stevens, B., Storch, J.-S., Tian, F., Voigt, A., Vrese, P., Wieners, K.-H., Wilkenskjeld, S., Winkler, A., and Roeckner, E.: Developments in the MPI-M Earth System Model version 1.2 (MPI-ESM1.2) and Its Response to Increasing CO 2, J. Adv. Model. Earth Syst., 11, 998–1038, https://doi.org/10.1029/2018ms001400, 2019.

Meccia, V. L. and Mikolajewicz, U.: Interactive ocean bathymetry and coastlines for simulating the last deglaciation with the Max Planck Institute Earth System Model (MPI-ESM-v1.2), Geoscientific Model Development, 11, 4677–4692, https://doi.org/10.5194/gmd-11-4677-2018, 2018.

Murray, T., Scharrer, K., Selmes, N., Booth, A. D., James, T. D., Bevan, S. L., Bradley, J., Cook, S., Llana, L. C., Drocourt, Y., Dyke, L., Goldsack, A., Hughes, A. L., Luckman, A. J., and McGovern, J.: Extensive retreat of Greenland tidewater glaciers, 2000–2010, Arctic, Antarctic, and Alpine Research, 47, 427–447, https://doi.org/10.1657/aaar0014-049, 2015.

North Greenland Ice Core Project members: High-resolution record of Northern Hemisphere climate extending into the last interglacial period, Nature, 431, 147–151, https://doi.org/10.1038/nature02805, 2004.

Riddick, T., Brovkin, V., Hagemann, S., and Mikolajewicz, U.: Dynamic hydrological discharge modelling for coupled climate model simulations of the last glacial cycle: the MPI-DynamicHD model version 3.0, Geoscientific Model Development, 11, 4291–4316, https://doi.org/10.5194/gmd-11-4291-2018, 2018.

Rignot, E., Casassa, G., Gogineni, P., Krabill, W., Rivera, A., and Thomas, R.: Accelerated ice discharge from the Antarctic Peninsula following the collapse of Larsen B ice shelf, Geophysical Research Letters, 31, https://doi.org/10.1029/2004gl020697, 2004.

Roberts, W. H. G., Valdes, P. J., and Payne, A. J.: Topography's crucial role in Heinrich Events, Proceedings of the National Academy of Sciences, 111, 16 688–16 693, https://doi.org/10.1073/pnas.1414882111, 2014.

Schannwell, C., Drews, R., Ehlers, T. A., Eisen, O., Mayer, C., and Gillet-Chaulet, F.: Kinematic response of ice-rise divides to changes in ocean and atmosphere forcing, The Cryosphere, 13, 2673–2691, https://doi.org/10.5194/tc-13-2673-2019, 2019.

Schiller, A., Mikolajewicz, U., and Voss, R.: The stability of the North Atlantic thermohaline circulation in a coupled ocean-atmosphere general circulation model, Climate Dynamics, 13, 325–347, https://doi.org/10.1007/s003820050169, 1997.

Sevestre, H. and Benn, D. I.: Climatic and geometric controls on the global distribution of surge-type glaciers: implications for a unifying model of surging, J. Glaciol., 61, 646–662, https://doi.org/10.3189/2015jog14j136, 2015.

Sevestre, H., Benn, D. I., Luckman, A., Nuth, C., Kohler, J., Lindbäck, K., and Pettersson, R.: Tidewater Glacier Surges Initiated at the Terminus, J. Geophys. Res. Earth Surf., 123, 1035–1051, https://doi.org/10.1029/2017jf004358, 2018.

Smith, R. S. and Gregory, J. M.: A study of the sensitivity of ocean overturning circulation and climate to freshwater input in different regions of the North Atlantic, Geophysical Research Letters, 36, n/a–n/a, https://doi.org/10.1029/2009gl038607, 2009.

Stouffer, R. J., Yin, J., Gregory, J. M., Dixon, K. W., Spelman, M. J., Hurlin, W., Weaver, A. J., Eby, M., Flato, G. M., Hasumi, H., Hu, A., Jungclaus, J. H., Kamenkovich, I. V., Levermann, A., Montoya, M., Murakami, S., Nawrath, S., Oka, A., Peltier, W. R., Robitaille, D. Y., Sokolov, A., Vettoretti, G., and Weber, S. L.: Investigating the Causes of the Response of the Thermohaline Circulation to Past and Future Climate Changes, Journal of Climate, 19, 1365–1387, https://doi.org/10.1175/jcli3689.1, 2006.

Straneo, F. and Heimbach, P.: North Atlantic warming and the retreat of Greenland's outlet glaciers, Nature, 504, 36–43, https://doi.org/10.1038/nature12854, 2013.

Tarasov, L. and Peltier, W.: Arctic freshwater forcing of the Younger Dryas cold reversal, Nature, 435, 662–665, https://doi.org/10.1038/nature03617, 2005.

https://doi.org/10.5194/egusphere-2022-332
Preprint. Discussion started: 30 May 2022

Ullman, D. J., LeGrande, A. N., Carlson, A. E., Anslow, F. S., and Licciardi, J. M.: Assessing the impact of Laurentide Ice Sheet topography on glacial climate, Clim. Past, 10, 487–507, https://doi.org/10.5194/cp-10-487-2014, 2014.

Weaver, A. J., Saenko, O. A., Clark, P. U., and Mitrovica, J. X.: Meltwater Pulse 1A from Antarctica as a Trigger of the Bølling-Allerød Warm Interval, Science, 299, 1709–1713, https://doi.org/10.1126/science.1081002, 2003.

Ziemen, F. A., Rodehacke, C. B., and Mikolajewicz, U.: Coupled ice sheet–climate modeling under glacial and pre-industrial boundary conditions, Climate of the Past, 10, 1817–1836, https://doi.org/10.5194/cp-10-1817-2014, 2014.

Ziemen, F. A., Kapsch, M.-L., Klockmann, M., and Mikolajewicz, U.: Heinrich events show two-stage climate response in transient glacial simulations, Climate of the Past, 15, 153–168, https://doi.org/10.5194/cp-15-153-2019, 2019.